

Oxidative Dehydrogenation on Nanocarbon: Identification and Quantification of Active Sites by Chemical Titration**

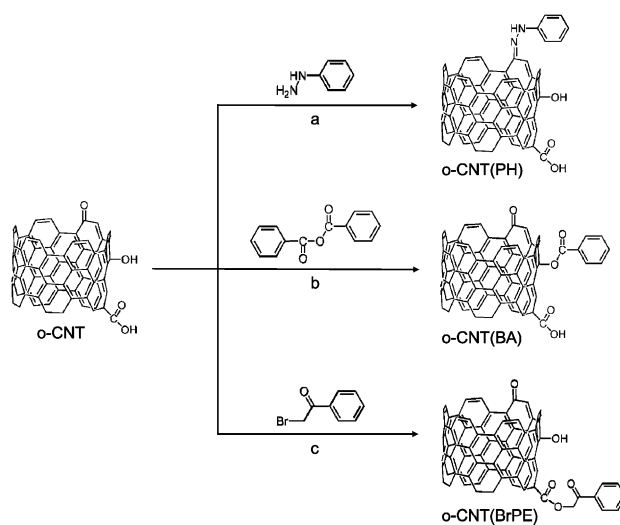
Wei Qi, Wei Liu, Bingsen Zhang, Xianmo Gu, Xiaoling Guo, and Dangsheng Su*

Nanostructured carbon-based materials have shown high catalytic activity in several important reactions and related chemical industrial processes, such as direct or oxidative dehydrogenation of hydrocarbons and Friedel–Crafts reactions.^[1] Nanocarbon materials exhibit significant advantages over traditional metal or metal oxide based catalysts because of their tunable acidity/basicity, electron density, and convenient recycling and reusability, and they have been shown to be potential alternatives to conventional catalysts to meet the requirements of sustainable chemistry.^[2] As a result, the field of nanocarbon catalysis has been experiencing an unparalleled development of new catalyst synthesis or their applications in new reaction systems. However, there is only slow growth of mechanistic interpretation of carbon-catalyzed reactions, which is even more urgent to advance our knowledge in related fields.^[2c,3]

Present research on the mechanism of carbon catalysis suggests that oxygen containing functional groups, especially ketonic carbonyl groups on nanocarbon, which are rich in electrons, may act as the catalytic active sites for oxidative dehydrogenation (ODH) of alkanes to corresponding alkenes.^[4] The reaction process is assumed to be similar to that for transition-metal oxide catalysts.^[5] The C–H bonds of alkanes dissociate at active oxygen functional groups, and the hydrogen atoms are abstracted by Lewis base sites. After the desorption of alkene products, gas-phase O₂ reacts with the abstracted hydrogen to form H₂O, then the active catalytic sites are regenerated to finish one catalytic cycle.^[6] The above unspecific catalytic mechanism is only based on the qualitative characterization of carbon catalysts, while the identity of the active sites or a detailed kinetic study has never been executed with direct and convincing chemical evidence. One of the most critical problems that limits the quantitative description of the catalytic mechanism is the uncertainty of the chemical structure of nanocarbon materials.^[7] The coexistence of several kinds of surface functional groups (such as

hydroxyl, carbonyl, and carboxylic acid groups) is unavoidable, as the synthesis or the following surface modification procedures of nanocarbon catalysts are normally realized by a severe physical or chemical process, such as laser irradiation and oxidation by HNO₃, O₂, and O₃.^[8] There are still lack of reliable quantification methods for the surface functional groups on nanostructured carbon materials because of their complexity in type and quantity.^[9] As a result, turnover frequency (TOF), the ultimate parameter to evaluate the intrinsic activity of heterogeneous catalysts, is also rarely reported in the case of nanocarbon catalysts, making it impossible to study the detailed reaction kinetics or compare the activity of carbon catalysts bearing different structures fairly and objectively. The quantitative surface composition analysis is also desirable for the application of nanostructured carbon as a catalyst support or electrochemical devices, which takes an even larger proportion in the field of carbon materials, as the surface structure of nanocarbon materials is essential for their physical or chemical properties (for example, affinity for a certain metal or metal ion).^[10]

In view of the quantification methods of oxygen functional groups,^[11] herein we propose a chemical titration method to determine the surface concentration of three kinds of typical oxygen functional groups (–C=O, –C–OH, and –COOH) on the surface of carbon nanotubes (CNTs) (Scheme 1). Through selective deactivation of these specific oxygen functional groups and the assessment of the catalytic activity of different CNT derivatives for ethylbenzene (EB) ODH reactions, we provided chemical evidence to show that



Scheme 1. The titration processes for a) ketonic carbonyl, b) phenol, and c) carboxylic acid groups on CNTs.

[*] Dr. W. Qi, W. Liu, Dr. B. Zhang, X. M. Gu, X. L. Guo, Prof. Dr. D. S. Su Shenyang National Laboratory for Materials Science Institute of Metal Research, Chinese Academy of Sciences Shenyang, 110016 (China) E-mail: dssu@imr.ac.cn

[**] The authors acknowledge the financial support from MOST (2011CBA00504), the NSFC of China (51221264, 21261160487, 21133010, 21303226, 21203215), a General Financial Grant from the China Postdoctoral Science Foundation (2012M520651), and a Tingsui Ke fellowship. The authors thank Prof. Dr. Robert Schlögl, Dr. Benjamin Frank, and Dr. Annette Trunschke from FHI (Berlin) and Prof. Dr. Garry Haller from Yale for fruitful discussions.



Supporting information for this article is available on the WWW under <http://dx.doi.org/10.1002/anie.201306825>.

ketonic carbonyl groups are the active sites on CNT catalysts in EB ODH reactions. TOFs for nanocarbon catalysts are provided for the first time based on the quantity of active sites determined by titration, which reflect the intrinsic catalytic activity of CNT catalysts.

Commercially available CNTs are first oxidized with concentrated HNO_3 (see the Supporting Information), and the oxidized samples are denoted as *o*-CNTs, which are mainly covered with phenol, carbonyl, carboxylic acid, carboxylic anhydride, and lactone groups on their surface.^[12,13] Phenylhydrazine (PH) is chosen as the titrant to quantify the content of ketonic carbonyl groups on *o*-CNTs (Scheme 1 a), because the reaction between hydrazine compounds and ketonic carbonyl groups is highly specific (forming hydrazones at a yield over 99.9%) under gentle reaction conditions.^[9,14] PH has similar molecular size, structure, and polarity to that of EB and is an appropriate candidate analogue to quantify the amount of carbonyl groups, which could possibly be contacted by and react with EB during the catalytic reaction. TEM images (Supporting Information, Figure S1) of *o*-CNT and the obtained CNT derivative (denoted as *o*-CNT(PH)) reveal that the shape and size distribution of *o*-CNTs are maintained after reacting with PH.

O-CNT and *o*-CNT(PH) exhibit similar N_2 adsorption isotherms (Figure S2) and an identical total pore volume and surface area (*o*-CNT: $1.18 \text{ cm}^3 \text{ g}^{-1}$, $219 \text{ m}^2 \text{ g}^{-1}$; *o*-CNT(PH): $1.18 \text{ cm}^3 \text{ g}^{-1}$, $222 \text{ m}^2 \text{ g}^{-1}$), indicating that there is no significant amount of physical adsorbed PH on CNT walls after derivatization. The Raman spectra of pristine CNTs, *o*-CNTs, and *o*-CNT(PH) (Figure S3) consists of two characteristic scattering modes: a D- (defect) and a G- (graphitic) band, respectively. The ratio between the intensity of D- and G-band (value of I_D/I_G) is conventionally known as an estimate of the content of defects or amorphous carbon adsorbents on CNTs.^[15,16] In our case, the value of I_D/I_G for *o*-CNTs is higher than that for raw CNTs (1.9 vs. 1.7), indicating an increase of surface defects owing to the aggressive reflux treatment in concentrated HNO_3 .^[17] On the other hand, the value of I_D/I_G for *o*-CNT(PH) is identical to that for *o*-CNTs (1.9 vs. 1.9), confirming that the derivatization process has no effect on defects.

The IR spectra of *o*-CNT(PH) exhibit a significant decrease of the $\text{C}=\text{O}$ signal at 1548 cm^{-1} compared to that of *o*-CNT, and there is also an obvious vibration mode emerged at 1840 cm^{-1} owing to the formation of $\text{C}=\text{N}$ bond during titration (Figure S4), indicating the successful reaction between PH and ketonic groups on CNTs. The peak area obtained through deconvolution of the $\text{O}1\text{s}$ XPS spectra reflects the relative surface concentration of different O species (Figure 1 a).^[18,19] The surface concentration of $\text{C}=\text{O}$ (ketonic carbonyl groups) drops by around 84% after reaction with PH, while the relative content of $\text{C}-\text{OH}$ (phenol groups) and $\text{O}=\text{C}-\text{O}$ (sum of carboxylic acid, anhydride, lactone, and ester groups) showed negligible changes during this process. Compared with *o*-CNTs, the $\text{N}1\text{s}$ XPS spectra (Figure 1 b) of *o*-CNT(PH) shows a significant peak owing to the formation of $\text{C}=\text{N}$ bonds (Scheme 1). The N content for *o*-CNT(PH) is 0.71% (atomic percent) from XPS measurement, and thus the surface concentration

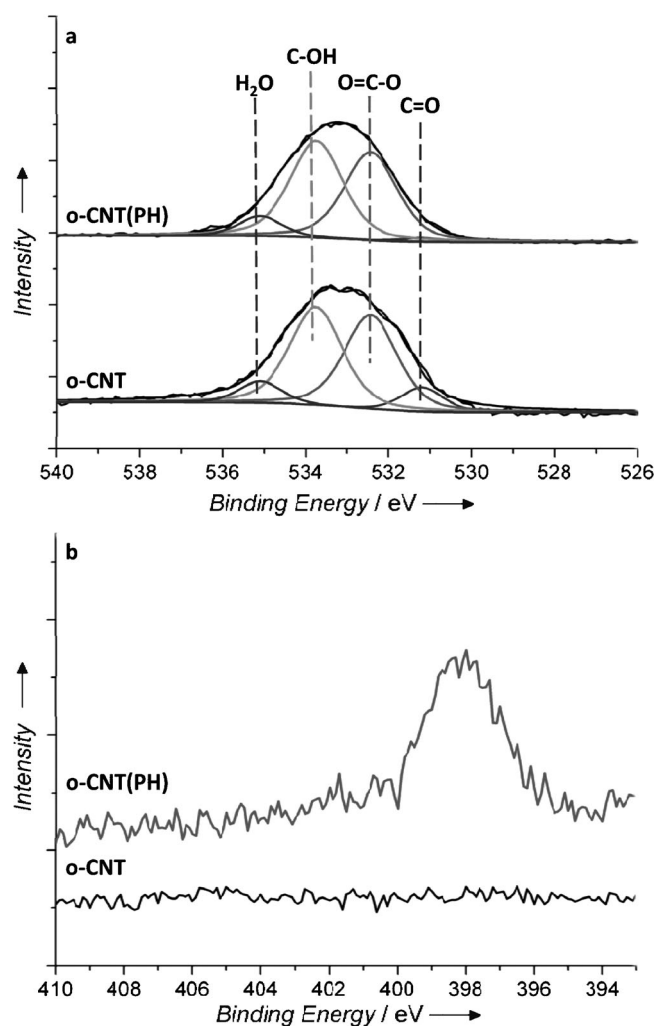


Figure 1. a) $\text{O}1\text{s}$ and b) $\text{N}1\text{s}$ XPS spectra of *o*-CNT (bottom) and *o*-CNT(PH) (top), respectively.

of $\text{C}=\text{O}$ groups that reacted with PH is around 0.8 CO nm^{-2} , as the reaction between PH and $\text{C}=\text{O}$ groups is considered to be a quantitative reaction (Scheme 1).^[14]

UV/Vis spectroscopy is also used to quantify the consumption of PH during the titration process. The CHCl_3 solution of PH exhibits two distinct absorption peaks at 249 and 288 nm, and both can be used to measure the quantity of PH molecules consumed in titration (Figure S5). The surface concentration of $\text{C}=\text{O}$ groups on *o*-CNT is 0.9 CO nm^{-2} obtained from the UV/Vis quantification measurement, which is consistent with that obtained from XPS analysis on *o*-CNT(PH) (0.8 CO nm^{-2}).

Utilizing the other two specific and quantitative reactions (Scheme 1 b,c), phenol^[11] and carboxylic acid^[20] groups on CNTs can also be titrated and deactivated, and the resulting CNT derivatives are named as *o*-CNT(BA), and *o*-CNT-(BrPE), respectively. As with the ketonic carbonyl groups, the surface concentration of phenol and carboxylic acid groups on CNTs can also be calculated through XPS or GC concentration analysis during titration. The surface concentration, obtained from these two independent measurements, shows

Table 1: Surface concentration of ketonic carbonyl, phenol, and carboxylic acid groups on CNTs.

Oxygen functional groups	Carbonyl	Phenol	Carboxylic acid
surface concentration ^[a]	0.8	6.9	1.3
surface concentration ^[b]	0.9	7.6	1.0

[a] Surface concentration: the number of oxygen functional groups normalized by surface area (groups/nm²), calculated from XPS measurements on corresponding CNT derivatives. [b] Surface concentration: the number of oxygen functional groups normalized by surface area (groups/nm²), calculated from UV/Vis or GC measurements on titrant during the titration process.

high consistency (Table 1), indicating the accuracy of the chemical titration method. Moreover, the results from independent control experiments, which were run with the titrants listed in Scheme 1 and small organic molecules (phenol, ketone, and carboxylic acid compounds), show that the selectivity of the titrant to corresponding oxygen functional group (for example, PH vs. C=O) are over 98% (Figure S6), and there is no obvious interference among oxygen functional groups, indicating that the reactions used in the titration process are highly selective in quantification and deactivation of a single functional group.^[9]

TPD-MS is used to verify the accuracy of the above titration method. Although it is difficult to obtain an absolute value of the surface concentration, the TPD profile (CO or CO₂) of *o*-CNTs could identify the oxygen functional groups and provide a ratio between some of them without uncertainty, as it is generally accepted that each type of oxygen functional group decomposes to a definite product (H₂O, CO, or CO₂) at a given temperature.^[21] The mole ratio of phenol and carbonyl groups existing on *o*-CNT is 9.2 ± 0.4 obtained by deconvolution of the CO TPD profile (Figure S7), consistent with the titration results (the corresponding ratio is 9.5), thus confirming the credibility of the surface concentration of oxygen functional groups obtained from above titration method.

The ODH reaction of EB is selected as a model reaction to evaluate the catalytic activity of *o*-CNTs and its derivatives (*o*-CNT(PH), *o*-CNT(BA), and *o*-CNT(BrPE)), that is, the contribution of corresponding oxygen functional groups (C=O, C-OH, and -COOH, respectively) to ODH reactions. The reaction is performed under relatively gentle conditions to ensure the structural integrity of CNT derivatives. The reaction temperature is chosen as 265 °C, which is below the decomposition temperature of CNT derivatives (above 300 °C from TG; Figure S8). XPS and elemental analysis performed on CNTs or their derivatives before and after 10 h of catalytic reaction provide identical structural information (element content and species), indicating *o*-CNTs and their derivatives are stable under the chosen conditions. Styrene is the main product (the selectivity for which is over 98%) of the EB ODH reaction under the catalysis of *o*-CNTs or their derivatives, and only a small amount of benzene and CO₂ is found as by-products from combustion. EB conversion rates on *o*-CNTs or CNT derivatives normalized by surface area (10^{-4} molecules nm⁻² s⁻¹) are first used to evaluate the catalytic activity of corresponding materials. As shown in

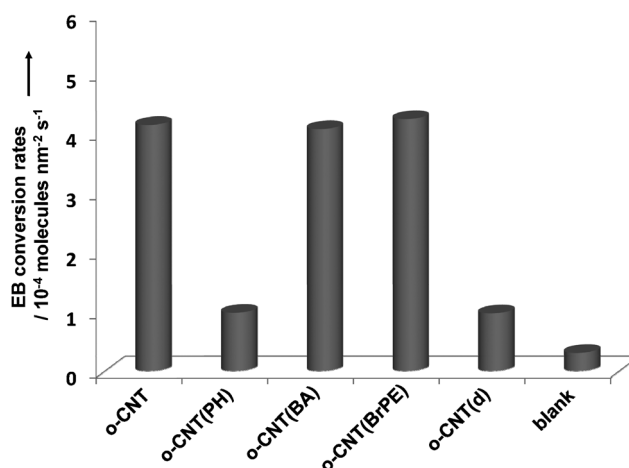


Figure 2. EB ODH conversion rates on *o*-CNTs, *o*-CNT derivatives, and CNTs with only defects. The blank reaction is run on equal weight of glass wool in the reactor. Reaction conditions: 538 K, 2.8 kPa EB, 1.4 kPa O₂, balance He, 100 mg catalyst.

Figure 2, the EB ODH catalytic activity of *o*-CNT(PH) is much lower (about 80%) than that of *o*-CNT under the same reaction condition, while the activity of *o*-CNT(BA) and *o*-CNT(BrPE) is similar to that of *o*-CNTs, indicating that the catalytic activity of *o*-CNTs exhibited in EB ODH reactions comes mainly from ketonic carbonyl groups. This result is consistent with in situ XPS measurements on the working surface of *o*-CNT catalysts, which shows that carbonyl groups are a critical ingredient of the active sites for ODH reactions.^[13]

A control experiment was run to clarify the origin of residual ODH catalytic activity of *o*-CNT(PH). The *o*-CNTs were first pre-treated in situ in Ar at 1300 °C for 30 min to remove all of the oxygen groups on their surface. These CNTs with only defects on their surface (named as *o*-CNT(d)) exhibit the same catalytic activity as that of *o*-CNT(PH) under the same reaction conditions (Figure 2; 0.86 vs. 0.85×10^{-4} molecules nm⁻² s⁻¹), indicating that the residual ODH catalytic activity of *o*-CNT(PH) may be attributed to the presence of defects on CNTs owing to HNO₃ treatment.^[17] XPS and elemental analysis results show that the content of oxygen on *o*-CNT(d) increases from 0 to around 2% after 10 h of EB ODH reaction, indicating the formation of oxygen functional groups on CNTs, as the chemically active defects easily chemisorbed oxygen and were oxidized under the reaction conditions.^[22] These newly formed oxygen functional groups existing on CNTs, in particular ketonic carbonyl groups, are considered as the active sites to catalyze EB ODH reactions, which are responsible for the residual ODH activity of *o*-CNT(PH).

The ODH activity of *o*-CNTs and *o*-CNT(PH) under various reaction conditions have also been evaluated and compared (Figure 3). *o*-CNT(PH) exhibit significantly lower (75–85%) ODH activity than *o*-CNTs under all of the conditions we used. The EB conversion rates on *o*-CNTs exhibit an approximately linear increase with increasing partial pressure of O₂; however, the corresponding rates on *o*-CNT(PH) reach a plateau at the O₂/EB ratio beyond 10,

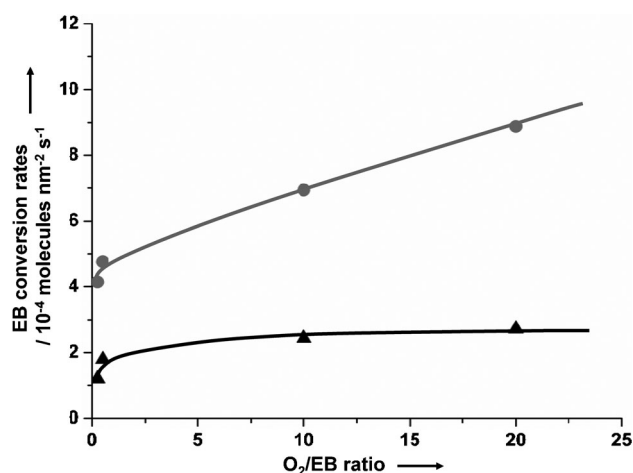


Figure 3. EB ODH conversion rates on *o*-CNTs (top, ●) and *o*-CNT(PH) (bottom, ▲) as a function of O_2/EB molar ratio. Reaction conditions: 538 K, 0.28–2.8 kPa EB, 0.12–5.6 kPa O_2 , and balance He, 100 mg catalyst.

suggesting that the residual ODH activity of *o*-CNT(PH) shows weak dependence on O_2 . This result is consistent with above hypothesis that the residual ODH activity of *o*-CNT(PH) comes from the newly generated carbonyl groups from the oxidation of defects, as the surface concentration of newly forming carbonyl groups is limited by the initial content of defects on *o*-CNT surface.

Finally, we correlated the ODH activity (EB ODH conversion rates) to the surface concentration of carbonyl groups. *o*-CNTs with various content of oxygen functional groups on their surface are obtained through adjusting the refluxing oxidation time (0.5–20 h) in HNO_3 ,^[12b] and the surface concentration of ketonic carbonyl groups are determined by chemical titration with PH as shown above. EB conversion rates exhibit a linear dependence on the surface concentration of carbonyl groups (Figure 4), further confirming that ketonic carbonyl groups are the active sites for carbon catalysis in ODH reactions. As shown in Figure 4, if the

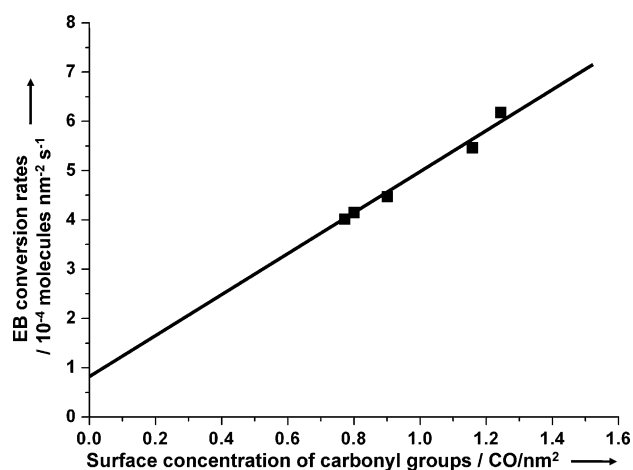


Figure 4. EB ODH conversion rates on *o*-CNTs with different surface concentration of carbonyl groups. Reaction conditions: 538 K, 2.8 kPa EB, 1.4 kPa O_2 , balance He, 100 mg catalyst.

surface concentration of carbonyl groups is extrapolated to zero, EB conversion rate intersects the y axis at a non-zero value, indicating that the catalytic activity (EB ODH rates) measured on *o*-CNTs comprises the contribution of defects as discussed above. Moreover, the value of EB conversion rate obtained through above extrapolation of ODH rates measured on *o*-CNTs, which could reflect the contribution of defects on EB ODH, is consistent with that independently measured on *o*-CNT(PH) or *o*-CNT(d) (0.82 vs. 0.86 and 0.85×10^{-4} molecules $nm^{-2} s^{-1}$), indicating that all the active sites (ketonic carbonyl groups) are accurately counted and deactivated through chemical titration with PH, and confirming the accuracy of the titration process. The slope of the line in Figure 4 represents the catalytic activity of single carbonyl group on *o*-CNTs after taking off the contribution of defects, namely the value of the TOF for *o*-CNTs normalized by the number of active sites, which reflects the intrinsic activity for an individual sample. The value of TOF is 4.1×10^{-4} molecules $CO^{-1} s^{-1}$, and is identical for all *o*-CNT samples used in the present research, as they share the same structure. This value seems a few orders smaller than TOF numbers usually found in heterogeneous catalysis,^[23] but matches very well the value reported by Figueiredo et al. for the same reaction.^[24]

In summary, we have proposed a novel chemical titration method to quantify three main types of oxygen functional groups (carbonyl, phenol, and carboxylic acid) on CNTs. Several independent measurements were conducted on CNT derivatives or the titration system to confirm that our titration method shows equivalent or even higher accuracy than traditional TPD or XPS methods. At the same time, the proposed chemical titration method can provide the absolute value of the surface concentration of oxygen functional groups and avoid the ambiguity and subjectivity brought by traditional spectroscopy based identification methods, and shows its unique advantage in quantification of oxygen functional groups on CNTs. More importantly, from the comparison of the catalytic activity of different CNT derivatives, we show, for the first time, direct chemical evidence that the active sites for carbon catalysis in ODH reactions are carbonyl groups. The ODH catalytic activity of CNTs is directly correlated with the surface concentration of ketonic carbonyl groups on CNTs. TOFs of CNTs during EB ODH reactions obtained from this method reflects the intrinsic activity of the catalyst, which provides a promising way to compare the activity of different carbon materials fairly, and sheds light on the quantitative description, the mechanism, and catalyst structure–function relationship for carbon catalysis.

Experimental Section

Chemical titration of oxygen functional groups on *o*-CNTs: For the titration of carbonyl groups on *o*-CNTs, PH (2 g) and hydrochloric acid (38 %, 100 μ L) were dissolved in $CHCl_3$ (100 mL), and then *o*-CNT (1 g) was added into the solution. After stirring for 72 h, the precipitate is filtered and washed with $CHCl_3$ in a Soxhlet extractor for 20 h. The precipitate was dried in vacuum at 60 °C for 24 h to give black carbon nanotube derivatives (*o*-CNT(PH)). The titration of

phenol and carboxylic acid groups on *o*-CNT was performed by a similar procedure with BA and BrPE as titrants, respectively.

ODH catalytic activity measurement: EB ODH rates were measured on *o*-CNT or CNT derivative catalysts (0.1–0.2 g) at 538 K using tubular quartz flow reactor with plug flow. Reactant mixtures contained EB (99.9%, Fisher Scientific), O₂ (99.999%, Praxair), and He (99.999%, Praxair) at a typical gas flow rate of 6000 mL g^{−1} g_{cat}^{−1}, and the molar flow rates were adjusted to give the desired EB and O₂ pressures (0.28–2.8 kPa and 0.12–5.6 kPa, respectively). EB ODH rates are reported as the conversion rates of EB and are normalized by the surface area of the catalysts measured by N₂ adsorption or by the number of active sites.

Received: August 4, 2013

Published online: November 8, 2013

Keywords: active sites · catalysis mechanisms · heterogeneous catalysis · nanocarbon materials · oxidative dehydrogenation

- [1] a) N. Keller, N. I. Maksimova, V. V. Roddatis, M. Schur, G. Mestl, Y. V. Butenko, V. L. Kuznetsov, R. Schlögl, *Angew. Chem.* **2002**, *114*, 1962–1966; *Angew. Chem. Int. Ed.* **2002**, *41*, 1885–1888; b) F. Goettmann, A. Fischer, M. Antonietti, A. Thomas, *Angew. Chem.* **2006**, *118*, 4579–4583; *Angew. Chem. Int. Ed.* **2006**, *45*, 4467–4471; c) J. Bitter, *J. Mater. Chem.* **2010**, *20*, 7312–7321; d) B. Frank, R. Blume, A. Rinaldi, A. Trunschke, R. Schlögl, *Angew. Chem.* **2011**, *123*, 10408–10413; *Angew. Chem. Int. Ed.* **2011**, *50*, 10226–10230; e) H. Yu, F. Peng, J. Tan, X. Hu, H. Wang, J. Yang, W. Zheng, *Angew. Chem.* **2011**, *123*, 4064–4068; *Angew. Chem. Int. Ed.* **2011**, *50*, 3978–3982.
- [2] a) J. de J. D. Velásquez, L. M. C. Suárez, J. L. Figueiredo, *Appl. Catal. A* **2006**, *311*, 51–57; b) I. F. Silva, J. Vital, A. M. Ramos, H. Valente, A. M. B. Rego, M. J. Reis, *Carbon* **1998**, *36*, 1159–1165; c) D. Su, S. Perathoner, G. Centi, *Catal. Today* **2012**, *186*, 1–6.
- [3] D. Su, J. Zhang, B. Frank, A. Thomas, X. Wang, J. Paraknowitsch, R. Schlögl, *ChemSusChem* **2010**, *3*, 169–180.
- [4] J. Carlsson, M. Scheffler, *Phys. Rev. Lett.* **2006**, *96*, 1–4.
- [5] a) J. Marulanda in *Carbon Nanotubes*, InTech, Rijeka, **2010**; b) J. Prasek, J. Drbohlavova, J. Chomoucka, J. Hubalek, O. Jasek, V. Adam, R. Kizek, *J. Mater. Chem.* **2011**, *21*, 15872–15884.
- [6] B. Frank, J. Zhang, R. Blume, R. Schlögl, D. Su, *Angew. Chem.* **2009**, *121*, 7046–7051; *Angew. Chem. Int. Ed.* **2009**, *48*, 6913–6917.
- [7] H. Boehm, *Carbon* **2002**, *40*, 145–149.
- [8] a) S. T. Oyama, R. Radhakrishnan, M. Seman, J. N. Kondo, K. Domen, K. Asakura, *J. Phys. Chem. B* **2003**, *107*, 1845–1852; b) C. Werncke, C. Limberg, C. Knispel, S. Mebs, *Chem. Eur. J.* **2011**, *17*, 12129–12135.
- [9] a) L. Langley, D. Villanueva, D. Fairbrother, *Chem. Mater.* **2006**, *18*, 169–178; b) K. Wepasnick, B. Smith, J. Bitter, D. Fairbrother, *Anal. Bioanal. Chem.* **2010**, *396*, 1003–1014.
- [10] a) I. Kvande, J. Zhu, T. Zhao, N. Hammer, M. Ronning, S. Raaen, J. Walmsley, D. Chen, *J. Phys. Chem. C* **2010**, *114*, 1752–1762; b) M. Lee, A. Dillen, J. Bitter, P. de Jong, *J. Am. Chem. Soc.* **2005**, *127*, 13573–13582.
- [11] a) C. Larabi, E. Quadrelli, *Eur. J. Inorg. Chem.* **2012**, 3014–3022; b) K. Wepasnick, B. Smith, K. Schrote, H. Wilson, S. Diegelmann, D. Fairbrother, *Carbon* **2011**, *49*, 24–36; c) A. Setyan, J. Sauvaina, M. Rossi, *Phys. Chem. Chem. Phys.* **2009**, *11*, 6205–6217.
- [12] a) S. Kundu, Y. Wang, W. Xia, M. Muhler, *J. Phys. Chem. C* **2008**, *112*, 16869–16878; b) I. Gerber, M. Oubenali, R. Bacsa, J. Durand, A. Goncalves, M. Pereira, F. Jolibois, L. Perrin, R. Poteau, P. Serp, *Chem. Eur. J.* **2011**, *17*, 11467–11477.
- [13] J. Zhang, X. Liu, R. Blume, A. Zhang, R. Schlögl, D. Su, *Science* **2008**, *322*, 73–77.
- [14] D. Applequist, H. Babad, *J. Org. Chem.* **1962**, *27*, 288–290.
- [15] F. Tuinstra, J. Koenig, *J. Chem. Phys.* **1970**, *53*, 1126–1130.
- [16] I. Maciel, N. Anderson, M. Pimenta, A. Hartschuh, H. Qian, M. Terrones, H. Terrones, J. Campos-Delgado, A. Rao, L. Novotny, A. Jorio, *Nat. Mater.* **2008**, *7*, 878–883.
- [17] J. Zhang, H. Zou, Q. Qing, Y. Yang, Q. Li, Z. Liu, X. Guo, Z. Du, *J. Phys. Chem. B* **2003**, *107*, 3712–3718.
- [18] T. Okpalugo, P. Papakonstantinou, H. Murphy, J. McLaughlin, N. Brown, *Carbon* **2005**, *43*, 153–161.
- [19] See Ref. [12a].
- [20] N. Dementev, X. Feng, E. Borguet, *Langmuir* **2009**, *25*, 7573–7577.
- [21] a) T. G. Ros, A. J. van Dillen, D. C. Koningsberger, *Chem. Eur. J.* **2002**, *8*, 1151–1162; b) W. Xia, D. Su, A. Birkner, L. Ruppel, Y. Wang, J. Qian, C. Liang, G. Marginean, W. Brandle, M. Muhler, *Chem. Mater.* **2005**, *17*, 5737–5742.
- [22] a) C. G. Salzmänn, S. A. Llewellyn, G. Tobias, M. A. H. Ward, Y. Huh, M. L. H. Green, *Adv. Mater.* **2007**, *19*, 883–887; b) V. Datsyuk, M. Kalyva, K. Papagelis, J. Parthenios, D. Tasis, A. Siokou, I. Kallitsis, C. Galiotis, *Carbon* **2008**, *46*, 833–840.
- [23] M. Boudart, *Chem. Rev.* **1995**, *95*, 661–666.
- [24] M. F. R. Pereira, J. J. M. Orfao, J. L. Figueiredo, *Appl. Catal. A* **1999**, *184*, 153–160.